Available online at www.sciencedirect.com
ScienceDirect
Trans. Nonferrous Met. Soc. China 22(2012) 1606−1612
Transactions of Nonferrous Metals Society of China
www.tnmsc.cn

Microstructure evolution of Zn−8Cu−0.3Ti alloy during hot deformation

XU Xiao-qing, LI De-fu, GUO Sheng-li, WU Xiao-ping

Nonferrous Processing Division, General Research Institute for Nonferrous Metals, Beijing 100088, China

Received 10 August 2011; accepted 30 September 2011

Abstract: The hot deformation behavior of homogenized zinc alloy was investigated through uniaxial compression test on a Gleeble−1500 thermal-mechanical simulator within a temperature range of 230−380 °C and a strain rate range of 0.01−10 s^{-1}, the corresponding flow curves and their characters were determined and analyzed, and microstructures were studied by optical, SEM and TEM microscopy. The results indicated that the microstructure evolution of zinc alloy during hot deformation involves the spheroidization of the phase of $TiZn_{15}$, coarsening of the precipitated phase and dynamic recrystallization (DRX) of the phase of matrix, leading to the formation of the polyphase (η+ε+$TiZn_{15}$) structure. The spheroidization of the phase of $TiZn_{15}$ during hot deformation was beneficial to the particle nucleation stimulated and then promoted to DRX of matrix. The dynamic recrystallization grain size of the matrix phase decreased firstly and then increased with elevating the temperature, and the degree of DRX became more complete when the strain rate and strain became larger. Hot deformation accelerated the diffusion of Cu atom, which resulted in the coarsening of the precipitated phase. Thus, the microstructure was refined owing to the pinning effect of the precipitated phase.
Key words: zinc alloy; dynamic recrystallization; high temperature deformation; polyphase alloy

1 Introduction

Peritectic alloys have been targeted as the most appealing engineering materials in recent years. Peritectic reactions involve one solid phase reacting with a liquid phase during cooling to generate a second solid phase, and are displayed in many alloy systems, such as steels, Cu alloys and titanium alloys. Extensive and systematic research efforts have been devoted to the solidification process of these alloys by many groups[1−5]. Zn−Cu alloy is a typical peritectic alloy, and is the most promising candidate of machined, pressed, and structural items due to its comparatively high strength and hardness. Additionally, Zn−Cu alloy has also been introduced into a series of daily commercial electronic products owing to its excellent electrical performance and shielding capability [1]. As a result of the low melting temperature and good casting property, zinc alloy has received rapid and comprehensive development. The microstructure evolution and phase selection have been investigated at different copper contents and under various solidification rates by many researchers in the past decades. Meanwhile, relatively mechanical and thermal-physical parameters have been measured [1,4−9], and thereby the simulated models have been established for the solidification process of Zn−Cu alloy [10].

Many efforts have been done for Zn−Cu alloys, preferably the cast Zn−Cu alloys. However, there are few reports on the deformed Zn−Cu alloy. Recently, the predictions of the microstructure and properties for deformed alloys have become one of the hotspots in the material science research, especially the investigation of microstructure evolution due to its determination to the alloys property [11−13]. Herein, in the present work uniaxial compression test of Zn−8Cu−0.3Ti was conducted. The microstructure evolution under different deformation conditions (temperature, strain rate and strain) was researched by optical microscopy (OM), scanning electron microscopy (SEM), X-ray diffraction (XRD) and transmission electron microscopy (TEM).

2 Experimental

The material used in the present study was commercial zinc alloy billet from Ningbo Powerway Alloy Materials Co., Ltd., China, with a composition of Zn−8Cu−0.3Ti (mass fraction, %). The homogeneous annealing was carried out in the air at 400 °C for 12 h to

Foundation item: Project (2009BAE71B03) supported by the National Key Technology Support Program of China During the 11th Five-year Plan Period
Corresponding author: LI De-fu; Tel: +86-10-82241292; E-mail: Lidf@grinm.com
DOI: 10.1016/S1003-6326(11)61363-0

eliminate the microstructure segregation. Figures 1 and 2 display the pristine microstructure composed of white equiaxial ε phase, bone-like $TiZn_{15}$ phase and gray matrix η phase. The annealed Zn−8Cu−0.3Ti alloy was machined to cylindrical specimens with a diameter of 8 mm and a height of 12 mm.

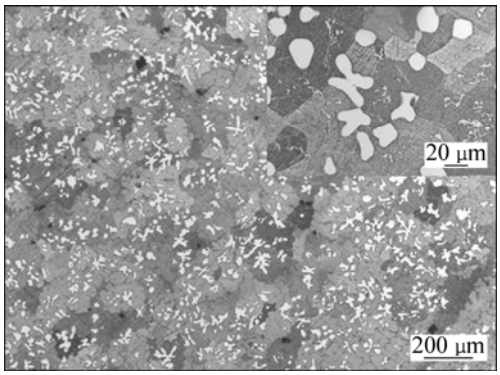

Fig. 1 Optical image showing microstructure of homogenized zinc alloy

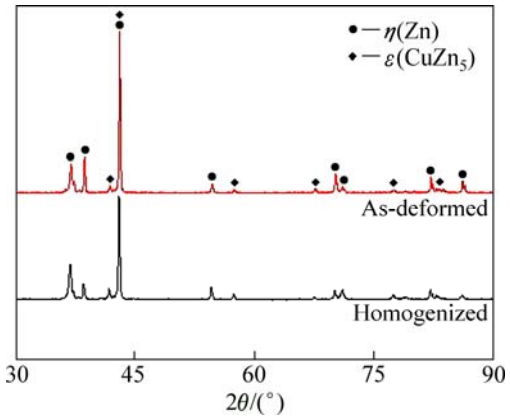

Fig. 2 XRD patterns of Zn−8Cu−0.3Ti zinc alloy

Hot compressive deformation simulation was performed on a Gleeble−1500 thermo-simulation machine. Graphite flake was used to eliminate the nonhomogeneity of temperature and the friction between specimen and the anvil. The temperature was measured by a thermocouple in the middle of specimen in real time. The specimen was firstly heated to 200 °C at a velocity of 5 °C/s, then to the deformation temperature at the speed of 3 °C/s followed by a 3 min heat preservation before compression. The deformed specimens were water quenched after compression to maintain the microstructure for observation because the water quenching was sufficient to inhibit the occurrence of static recrystallization. Deformation temperature ranged from 230 °C to 380 °C at the strain rates of 0.01, 0.1, 1 and 10 s^{-1}. The specific strains were 0.3, 0.5，0.7，0.9 and 1.2. The deformed specimens were then sectioned parallel to the axis, polished and then etched. The microstructure observation was performed with an Axiovert 200MAT optical microscope and HITACHI−S4800 scanning electron microscope. X-ray diffraction (XRD) patterns were obtained on a Rigaku D/MAX 2000 PC diffractometer operating at 40 kV and 25 mA, using Cu K_α radiation (λ=1.5406 Å).

3 Results and discussion

3.1 Flow stress characteristics of Zn−8Cu−0.3Ti zinc alloy

Figure 3 illustrates the true stress—strain curves in temperature range of 230−380 °C at a fixed strain rate of 1 s^{-1} and at a fixed temperature of 320 °C in a strain rate range of 0.01−10 s^{-1}, which exhibits a typical characteristic behavior of dynamic recrystallization. At the initial stage, the flow stress increased rapidly with the increase of the strain and reached the peak stress, then the stress decreased to a steady stress with the increase of the strain. Simultaneously, Figure 3 reveals that the steady stress and peak stress increase with the decrease of deformation temperature at a given strain rate of 1 s^{-1} and decrease with the increase of strain rates at a given deformation temperature of 320 °C.

During the deformation process the material

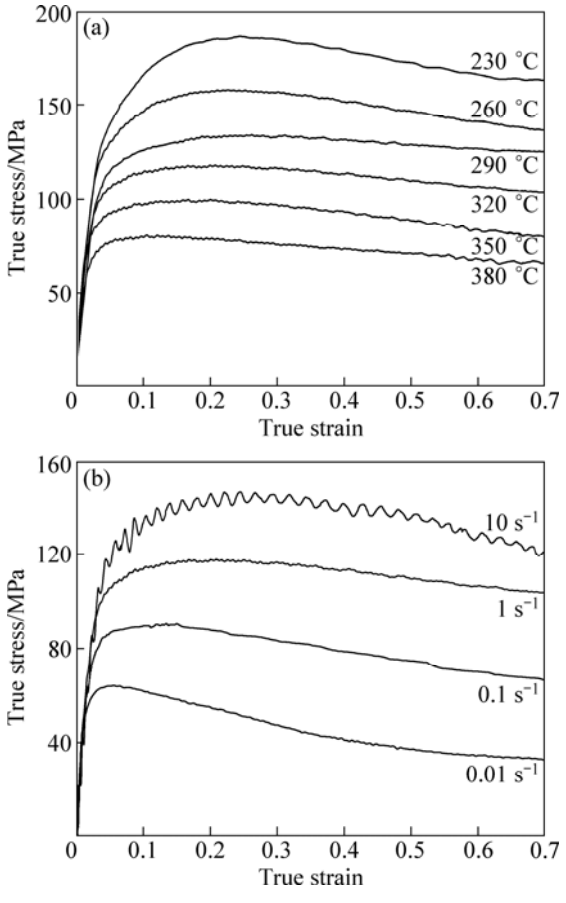

Fig. 3 True stress—true strain curves of Zn−8Cu−0.3Ti zinc alloy during hot compression deformation: (a) $\dot{\varepsilon}$ =1 s^{-1}; (b) t=320 °C

undergoes work hardening and thermally activated softening, which contribute to the three stages of true stress—strain curves shown in Fig. 3: stage I (work hardening stage), stage II (yielding stage), and stage III (steady stage) [14−16]. It can be seen that the characteristics of true stress — strain curves were fluctuant at 320 °C and 10 s^{-1} in Fig. 3(b). It probably is assigned to the interactive effect of DRX softening and work hardening [17,18].

True stress—strain curves at the strain rate of 1 s^{-1} shown in Fig. 3(a) show that the peak stress rose from 80 MPa at 380 °C to 187 MPa at 230 °C, when peak strain rose from 0.12 at 380 °C to 0.245 at 230 °C. It is assigned to the evaluation of temperature which lowered the resistance of the dislocation motion and facilitated the deformation. Meanwhile, the atom thermal vibration and dislocation motion were aggravated, which reduced the atomic interaction force and the critical shearing stress. Subsequently, more slip systems were triggered, which enhanced the matrix DRX and thereby reduced the flow stress.

True stress—strain curves at 320 °C shown in Fig. 3(b) reveal that the peak stress and flow stress increase with elevating the strain rate. This is attributed to the increase of strain rate which diminished the deformation time, and thus the accelerated dislocation motion speed induced plentiful multiplication and entanglement of dislocation. Eventually, the flow stress was increased. TEM image of the alloy after deformation under 260 °C and 1 s^{-1} is shown in Fig. 4(a). Pristine deformed grains

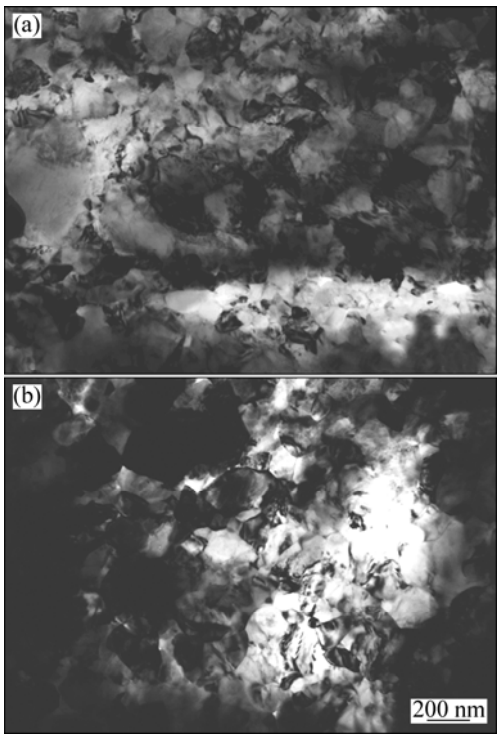

Fig. 4 TEM images of specimens compressed under different conditions: (a) 260 °C, 1 s^{-1}; (b) 380 °C, 1 s^{-1}

existed abundantly while plentiful dislocation presented at grain boundaries and sub-grains interior. Therefore, the 260 °C curve in Fig. 3(a) is comparatively high. Pristine deformed grains disappeared when the temperature was elevated to 380 °C, as shown in Fig. 4(b). Sub-grains grew up and the inside dislocations were annihilated, which resulted in the rapid decrease of flow stress.

3.2 Microstructure evolution of Zn−8Cu−0.3Ti alloy during deformation process

The microstructure evolution during hot deformation was not only affected directly by deformation process conditions (temperature, strain rate, strain) [19], but also controlled by the difference of alloy systems. It can be concluded that Zn−8Cu−0.3Ti alloy was composed of primary ε phase, bone-like $TiZn_{15}$ phase and matrix η phase from the optical microscopy (Fig. 1), the XRD pattern (Fig. 2) and the EDS spectrum (not given here). It is arduous to elucidate the microstructure evolution characteristic of Zn−8Cu−0.3Ti alloy owing to the different deformation mechanism and poor deformation compatibility of the phases [20].

3.2.1 Effect of deformation temperature

Figure 5 displays the deformed microstructures under different temperatures at strain rate of 1 s^{-1} and strain of 0.7. The original ε phase was flexural deformed vertically to the compression direction. Spheroidization and fracture occurred in the bone-like $TiZn_{15}$ phase also vertical to the compression direction. When the temperature was bellow 260 °C, the matrix η phase presented necklace-like structure composed of elongated initial grains and DRX grains. With the temperature elevated above 290 °C, the DRX degree was further enhanced, and the matrix was composed of abundant fine equiaxial DRX grains and a few elongated initial grains. Complete DRX took place with an average grain size of 5 μm when the temperature was elevated to 380 °C. The microstructure evolution with the temperature resulted from the thermal activated softening mechanism as discussed above.

Fine grains due to discontinuous dynamic recrystallization (DDRX) distributed at the initial grain boundaries and phase boundaries, which are marked with the black arrows in Fig. 5(a). The reason why DDRX grains appeared at the above mentioned place was that it provided the formation conditions for both high angle grain boundary (HGB) and high density of defects, which were in favor of the storage of deformation energy and the formation of DDRX nuclei [19].

The bone-like $TiZn_{15}$ phase was spheroidized with a size of 2.5−5 μm, of which stimulation effect on DRX could be elucidated by particle stimulate nucleation (PSN). The PSN was ascribed to the mechanical property

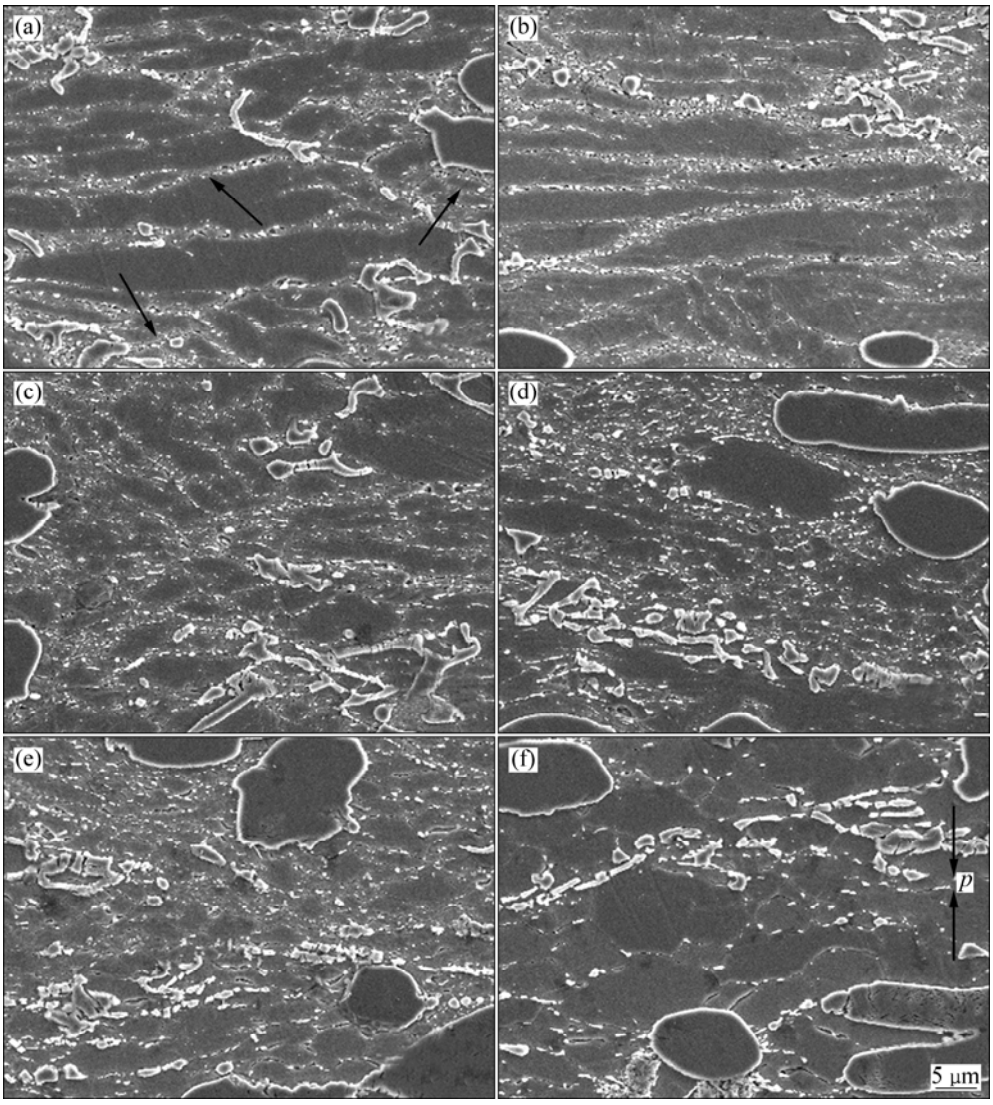

Fig. 5 SEM images showing microstructure evolution of zinc alloy deformed at strain rate of 1 s^{-1} and strain of 0.7 at different temperatures: (a) 230 °C; (b) 260 °C; (c) 290 °C; (d) 320 °C; (e) 350 °C; (f) 380 °C

discrepancy between phases. To coordinate the plastic deformation, large strain gradient formed around the big particles, which finally promoted the DRX nucleation. $TiZn_{15}$ phase acted as a hard barrier during the deformation process due to the incoherent relationship between matrix η phase and $TiZn_{15}$ phase. The barriers hindered the motion of dislocations and the further deformation of η phase. Therefore, the high dislocation density areas and high orientation gradient appeared in the matrix phase nearby the $TiZn_{15}$ phase, where was the favorable position of DRX nucleation. With the elevation of temperature, the spheroidization of $TiZn_{15}$ phase was more complete and the dislocation motion was fiercer, which provided more PSN nuclei and thereby stimulated the DRX. However, the DRX grains grew up slightly and the grain boundaries straightened when the temperature elevated to 380 °C [20].

3.2.2 Effect of strain rate

Figure 6 displays the deformed microstructures under different strain rates at 320 °C and strain of 0.7. When the strain rate was below 1 s^{-1}, the DRX grains were finer and volume fraction of DRX was larger with the increase of the strain rate. However, the grains grew up when the strain rate reached 10 s^{-1}. This phenomenon was attributed to the competition of two mechanisms. One was that the decrease of strain rate enhanced the diffusion and adjustment of atoms, lowered the accumulated dislocation density, and thereby diminished the DRX nuclei quantities; meanwhile, the lower strain rate was capable of the migration of grain boundaries and the growth of the DRX grains. The other one was that many fine white ε phases precipitated at the grain boundaries during deformation, as shown in Fig. 6. The new formed phase pinned the grain boundaries, slowed down the mobility of grain boundaries, and effectively blocked the growth of the DRX grains. Therefore, the

DRX degree of the zinc alloy was jointly influenced by the dislocation density and the precipitated phase.

Figure 6(a) (at strain rate of 0.01 s^{-1}) displays that the precipitated ε phase mainly distributed along the perpendicular direction to the compression direction with long ribbon-like shape of 4−6 μm. Additionally, a very small quantity of particles with size less than 1 μm dispersedly precipitated at the grain boundaries. When the strain rate was fixed at 0.1 s^{-1} as presented in Fig. 6(b), the precipitated white ε phase was generally less than 1 μm in size, and uniformly dispersed at the matrix grain boundaries. Only a few ribbon-like precipitated phase particles were observed. Besides, kinks and fusing spheroidization were observed in $TiZn_{15}$ phase vertically to the compression direction. The microstructure at 1 s^{-1} (Fig. 5(d)) exhibited that the sizes of the precipitated phase particles were all less than 1 μm but the quantities started reducing. As the strain rate rose to 10 s^{-1} in Fig. 6(c), the precipitated ε phase was comprised of particles all less than 1 μm, and the amount was greatly reduced. This was because the high strain rate confined the diffusion of Cu atom to the grain boundaries, which decreased the precipitation of fine dispersing ε phase. Accordingly, the pinning effect of precipitated phase to the grain boundaries was weakened, leading to the growth up phenomenon of the grains.

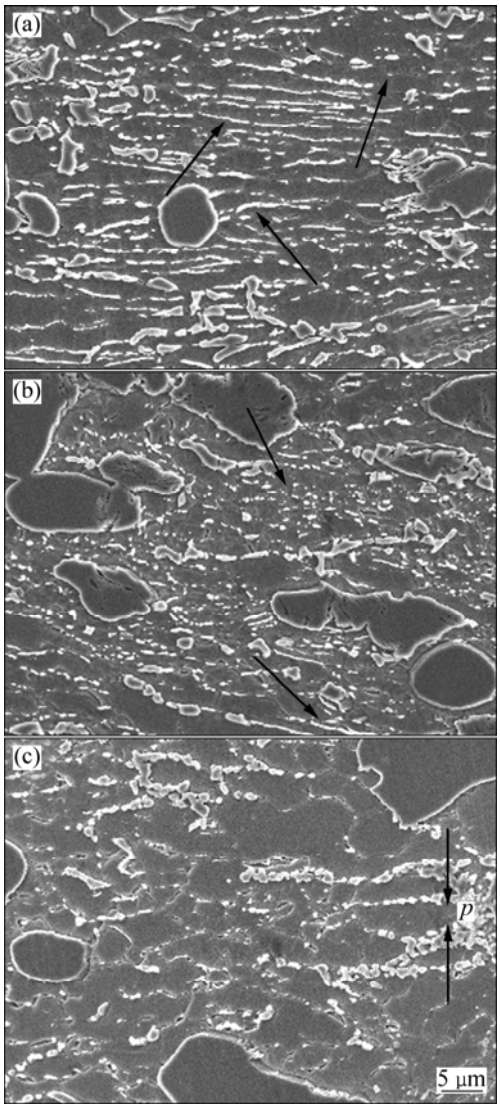

Fig. 6 SEM images showing microstructure evolution of zinc alloy deformed at 320 °C and strain of 0.7: (a) $\dot{\varepsilon}$=0.01 s^{-1}; (b) $\dot{\varepsilon}$=0.1 s^{-1}; (c) $\dot{\varepsilon}$=10 s^{-1}

From the above analysis, it was concluded that the influence of strain rate on the deformed microstructure should be considered to determine the deformation technics, preferably not more than 1 s^{-1}.

3.2.3 Effect of strain

It is obvious that complicated microstructure occurred and ultra-fined composite phases finally formed during the deformation process of the Zn−8Cu−0.3Ti alloy. The deformation process includes the spheroidization of the bone-like $TiZn_{15}$ phase, the precipitation of $CuZn_5$ phase and the DRX of the matrix η phase. To further make clear the microstructure evolution during the deformation process, the deformed microstructures at different strains were investigated and the probable deformation mechanism was discussed.

The microstructure evolution of Zn−8Cu−0.3Ti alloy at different strains under 320 °C and 0.1 s^{-1} is shown in Fig. 7. $TiZn_{15}$ phase began bending and even kinking at part larger curvature place when the strain reached 0.3, as displayed in Fig. 7(a). At the same time, quantities of $CuZn_5$ phase ribbons with length of 5−15 μm precipitated near the bone-like $TiZn_{15}$ phase layers and distributed at the originally deformed grain boundaries vertical to the deformation direction. Due to the existence of large scale $TiZn_{15}$ phase and its spheroidization, PSN occurred in the high density dislocation η phase matrix, and therefore DRX grains were observed in some place. Moreover, sphere-like $CuZn_5$ phase with size less than 1 μm precipitated at the grain boundaries which efficiently blocked the growth of the DRX grains. Further spheroidization of $TiZn_{15}$ phase was observed with the strain increased to 0.5 (Fig. 7(c)), and complete ribbon-like $TiZn_{15}$ phase disappeared at this time. The increase of the spheroidization particles enlarged the phase boundary energy which further accelerated the DRX of the η phase. The thorough spheroidizaiton of $TiZn_{15}$ phase was accomplished with a maximum size less than 3 μm when the strain rose to 0.9. The sphere-like $CuZn_5$ phase precipitated at the DRX grain boundaries was coarsened with size somewhat decreased. This phenomenon was assigned to the increase of activation energy which made the Cu atom precipitate preferably at the DRX grain boundaries and finally resulted in the coarsening [21]. Figure 7(d) presents the microstructure at the strain of 1.2, which proved that 90% of matrix η phase underwent the DRX

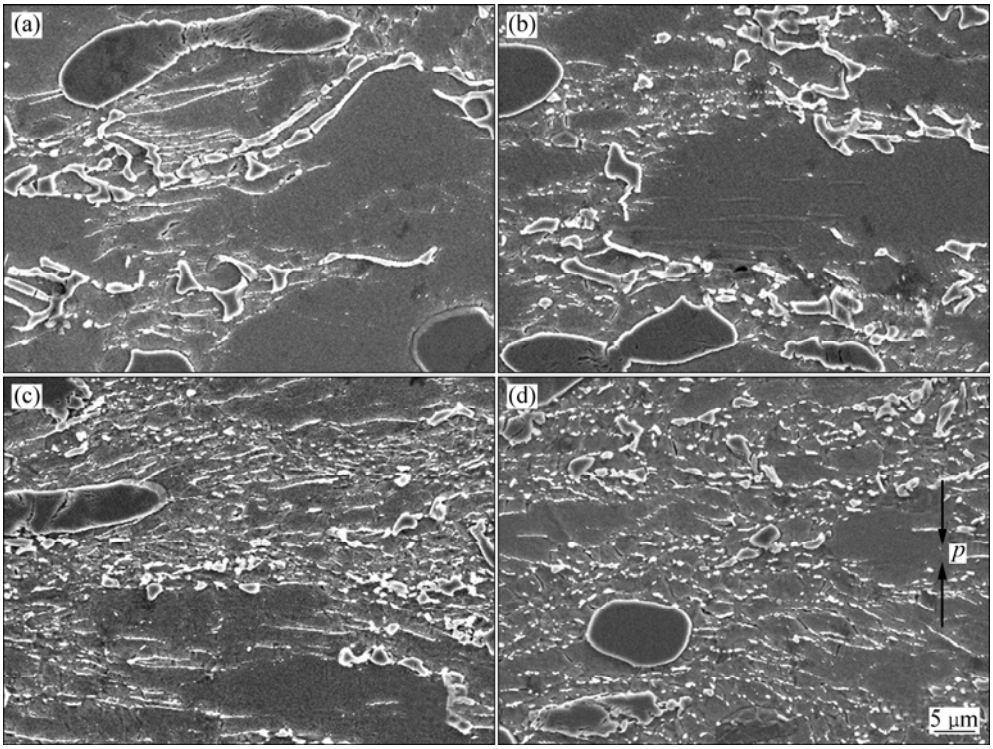

Fig. 7 SEM images showing microstructure evolution of zinc alloy deformed at 320 °C and 1 s^{-1}: (a) ε=0.3; (b) ε=0.5; (c) ε=0.9; (d) ε=1.2

with straight and distinct grain boundaries. Furthermore, great part of the bone-like microstructure was spheroidized except a very few regions.

4 Conclusions

1) When homogenized Zn−8Cu−0.3Ti alloy was deformed at an elevated temperature, the work hardening stage, yielding stage and steady stage varied with the temperature and strain rate; the flow stress and its peak value decreased with the increase of temperature and the decrease of strain rate.

2) Spheroidization occurred in the bone-like $TiZn_{15}$ phase during the deformation process, and the common border of it and the matrix was the favored site for DRX grain nuclei.

3) During the DRX process of the matrix, the $CuZn_5$ phase precipitated at the grain boundaries and effectively pinned the grain boundaries, which blocked the growth of the grains and finally made the ultra-fined composite microstructure obtained.

References

[1] KAYA H, CADIRLI E, ULGEN A. Investigation of the effect of composition on microhardness and determination of thermo-physical properties in the Zn−Cu alloys [J]. Materials and Design, 2011, 32: 900−906.

[2] HUNZIKER O, VANDYOUSSEFI M, KURZ W. Phase and microstructure selection in peritectic alloys close to the limit of constitutional undercooling [J]. Acta Materialia, 1998, 46(18): 6325−6336.

[3] LI Y, NG S C, MA D, JONES H. Observation of lamellar eutectic-like structure in a Zn−rich Zn−3.37%Cu peritectic alloy processed by Bridgman solidification [J]. Scripta Materialia, 1998, 39(1): 7−11.

[4] MA D, LI Y, NG S C, JONES H. Unidirectional solidification of Zn−rich Zn–Cu peritectic alloys—I. Microstructure selection [J]. Acta Materialia, 2000, 48(2): 419−431.

[5] MA D, LI Y, NG S C, JONES H. Unidirectional solidification of Zn-rich Zn–Cu peritectic alloys—II. Microstructural length scales[J]. Acta Materialia, 2000, 48(8): 1741−1751.

[6] MA D, XU W, NG S C, LI Y. On secondary dendrite arm coarsening in peritectic solidification [J]. Materials Science and Engineering A, 2005, 390(1−2): 52−62.

[7] XU W, FENG Y P, LI Y, ZHANG G D, LI Z Y. Rapid solidification behavior of Zn-rich Zn–Ag peritectic alloys [J]. Acta Materialia, 2002, 50: 183−193.

[8] WANG Meng, LIN Xin, SU Yun-peng, HUANG Dong-wei. Microstructure evolution in unidirectionalloy solidified Zn−Cu peritectic alloy I. Experiment and analysis [J]. Acta Metallurgica Sinica, 2003, 39(8): 831−837. (in Chinese)

[9] WANG Meng, LIN Xin, SU Yun-peng, HUANG Dong-wei. Microstructure evolution in unidirectionalloy solidified Zn−Cu peritectic alloy Ⅱ. Modification on the analysis [J]. Acta Metallurgica Sinica, 2003, 39(8): 838−842. (in Chinese)

[10] SU Yun-peng, WANG Meng, LIN Xin, CHEN Qian, HUANG Wei-dong. Numerical model for nucleation of peritectic alloy during unidirectional solidification [J]. J Mater Sci, 2007, 42: 5360−5368.

[11] LI Jun-peng, SHEN Jian, YAN Xiao-dong, MAO Bai-ping, YAN Liang-ming. Effect of temperature on microstructure evolution of 7075 alloy during hot deformation [J]. The Chinese Journal of Nonferrous Metals, 2008, 18(11): 1951−1957. (in Chinese)

[12] JAKOBSEN B, POULSEN H F, LIENERT U. Formation and subdivision of deformation structures [J]. Science, 2006, 312: 889−892.
[13] HIRSCH J. Thermomechanical control in aluminium sheet production [J]. Materials Science Forum, 2003, 426(1): 185−194.
[14] TENG Hao, YIN Zhi-min, ZHU Zhi-yuan, ZHOU Ke-chao, LI Zhi-you. Hot deformation behavior of Ni76Cr19AlTi superalloy [J]. Acta Metallurgica Sinica, 2006, 42(6): 629−634. (in Chinese)
[15] ZHANG Yi, LIU Ping, TIAN Bao-hong, CHEN Xiao-hong, JIA Shu-guo, REN Feng-zhang, LONG Yong-qiang. Dynamic recrystallization behavior of Cu−Ni−Si−P alloy [J]. The Chinese Journal of Nonferrous Metals, 2008, 18(7): 1242−1247. (in Chinese)
[16] CHEN Li-qing, ZHAO Yang, XU Xiang-qiu, LIU Xiang-hua. Dynamic recrystallization and precipitation behavior of a kind of low carbon V-microalloyed steel [J]. Acta Metallurgica Sinica, 2010, 46(10): 1215−1222. (in Chinese)
[17] SHEN Kun, WANG Ming-pu, GUO Ming-xing, LI Shu-mei. Study on high temperature deformation characteristics of Cu−0.23%Al_2O_3 dispersion-strengthened copper alloy [J]. Acta Metallurgica Sinica, 2009, 45(5): 597−604. (in Chinese)
[18] PAUL B, KAPOOR R, CHAKRAVARTTY J K, BIDAYE A C, SHARMA L G, SURI A K. Hot working characteristics of cobalt in the temperature range 600−950 °C [J]. Scripta Materialia, 2009, 60(2): 104−107.
[19] ZHANG Bei-jiang, ZHAO Guang-pu, XU Guo-hua, FENG Di. Hot deformation behavior and microstructure evolution of superalloy GH742 [J]. Acta Metallurgica Sinica, 2005, 41(11): 1207−1214. (in Chinese)
[20] WANG Meng, LI Long-fei, SUN Zu-qing. Effect of cementite particle size on dynamic recrystallization of ferrite in a low carbon steel [J]. Acta Metallurgica Sinica, 2007, 43(10): 1009−1014. (in Chinese)
[21] CHEN Wei, LI Long-fei, YANG Wang-yue, SUN Zu-qing, HE Jian-ping. Microstructure evolution of hypereutection steels during warm deformation I: Formation of equiaxial ferrite and effects of Al [J]. Acta Metallurgica Sinica, 2009, 45(2): 151−155. (in Chinese)

Zn−8Cu−0.3Ti 锌合金热变形的组织演变

许晓庆，李德富，郭胜利，邬小萍

北京有色金属研究总院 有色金属加工事业部，北京 100088

摘 要：利用 Gleeble−1500 热力模拟试验机在温度 230~380 °C，应变速率 0.01~10 s^{-1} 的条件下进行均匀化态 Zn−8Cu−0.3Ti 锌合金的热压缩变形实验，测定真应力—真应变曲线，利用 OM、SEM 和 TEM 对变形组织进行分析。结果表明：在变形过程中该合金发生了 $TiZn_{15}$ 相的球化、析出相的粗化和基体 η 相的动态再结晶，形成了(η+ε+$TiZn_{15}$)复相组织。变形过程中 $TiZn_{15}$ 相的球化有助于粒子协同方式实现粒子激发形核，有利于基体动态再结晶的发生。随着压缩变形温度的升高，基体动态再结晶晶粒的尺寸先减小后增大；随着应变速率和应变量的增大，动态再结晶进行得更充分；形变促进 Cu 原子的扩散，导致析出相的粗化，析出相的钉扎作用使组织得到细化。

关键词：锌合金；动态再结晶；高温变形；复相组织

(Edited by YANG Hua)